IEEE Access
Multidisciplinary | Rapid Review | Open Access Journal

Date of publication xxxx 00, 0000, date of current version xxxx 00, 0000.

*Digital Object Identifier 10.1109/ACCESS.2017.DOI*

# Functional Situational Awareness for Reliable and Efficient Operation of Hybrid Electric Vehicle Power Systems

**CHIRATH PATHIRAVASAM[1], (Student, IEEE), GANESH K. VENAYAGAMOORTHY[1], (Fellow, IEEE), RAJAN RATNAKUMAR[1], (Student, IEEE), and KYLE SKEEN[1], (Student, IEEE)**

[1]Real-Time Power and Intelligent Systems Laboratory, Holcombe Department of Electrical and Computer Engineering, Clemson University, Clemson, SC 29634, USA (e-mail: chirathd@ieee.org, gkumar@ieee.org)

Corresponding author: Chirath Pathiravasam (e-mail: chirathd@ieee.org).

This work was supported by the Simulation Based Reliability and Safety Program for modeling and simulation of military ground vehicle systems, under the technical services contract No. W56HZV-17-C-0095 with the U.S. Army DEVCOM Ground Vehicle Systems Center (GVSC), the National Science Foundation (NSF) of the United States, under grants IIP 1312260 and CNS 2131070, and the Duke Energy Distinguished Professorship Endowment Fund. Any opinions, findings and conclusions or recommendations expressed in this material are those of author(s) and do not necessarily reflect the views of GVSC, NSF and Duke Energy. Distribution A. Approved for public release; distribution unlimited. (OPSEC 7118)

**ABSTRACT** Hybrid electric vehicle power systems (VPSs) comprise of limited energy resources and variable load requirements. The functional status of components and subsystems that make up the VPS is critical to the overall system operation. The degradation and critical operating states of components affect system efficiency and reliability differently. Therefore, monitoring of the functional status (referred to as functional situational awareness (FSA)) of components, subsystems and system is needed for reliable and efficient operation of VPS. In this study, VPS-FSA is inferred hierarchically at three levels of complexity, namely, at the component, subsystem and system level. In each of these levels, two types of FSA are inferred to qualify and quantify the functional states of components, subsystems and system.
Component-FSA is based on currents and temperatures measurements of the components. Subsystem-FSA and System-FSA are derived as fusion of Component-FSA and Subsystem-FSA, respectively. Type 1-FSA is inferred using reasoning and threshold values. Type 2-FSA is derived using more complex relationships of temperature and current states. Typical FSA results are presented for a VPS for a standard drive cycle and long-term effects on the VPS operation are shown over several drive cylces.

**INDEX TERMS** Functional situational awareness, hybrid electric vehicles power system, component degradation, critical operating states.

## NOMENCLATURE

| | |
|---|---|
| $\alpha_{Com}$ | $Com$ criticality coefficient for current |
| $\beta_{Com}$ | $Com$ criticality coefficient for temperature |
| $\Delta D_{Com}$ | Degradation of $Com$ in a time step |
| $\Delta D_{Com,cyc}$ | Cycling degradation of $Com$ in a time step |
| $\Delta D_{Com,cal}$ | Calendar degradation of $Com$ in a time step |
| $\eta_{ini,com}$ | Initial efficiency of $Com$ |
| $\eta_{fin,com}$ | Final efficiency (at 100% degradation) of $Com$ |
| $\nu$ | Vehicle speed |
| $a_{com}$ | coefficient related to the mass and heat capacity of $Com$ |
| $b_{com}$ | coefficient related to he effective cross area and thermal conductivity of $Com$ |
| $Bat$ | Battery |
| $C_{Com}$ | Criticality estimation of $Com$ |
| $Com$ | Component |
| $D_{Com}$ | Degradation estimation of $Com$ |
| $D_{Com,A}$ | Lower degradation threshold of $Com$'s degraded state |
| $F_y^0$ | Functional state of $y$ |
| $F_y^{1,C}$ | Type 1 critical state of $y$ |
| $F_y^{1,D}$ | Type 1 degraded state of $y$ |
| $F_y^{1,N}$ | Type 1 normal state of $y$ |
| $F_y^{2,C}$ | Type 2-Criticality FSA of $y$ |
| $F_y^{2,D}$ | Type 2-Degradation FSA of $y$ |

| | |
|---|---|
| $Gen$ | Generator |
| $I_{Com}$ | Current measurement of $Com$ |
| $I_{Com,A}$ | Lower threshold $Com$'s critical current range |
| $I_{Com,NF}$ | Upper threshold $Com$'s critical current range |
| $k_{Com}$ | $Com$'s degradation coefficient |
| $L1$ | Electric load 1 |
| $L2$ | Electric load 2 |
| $Mot$ | Motor |
| $PCMi$ | Power converter module of subsystem $i$ |
| $P_x$ | Power consumption/ supply of $x$ (component or subsystem) |
| $Q_{l,com}$ | Heat loss of $Com$ |
| $Q_{c,com}$ | Cooling (heat rejection) of $Com$ |
| $SOC$ | Battery state of charge |
| $SS, i$ | Subsystem $i$ |
| $Sys$ | System |
| $t$ | time (present) |
| $T$ | True (boolean) |
| $T_{amb}$ | Ambient temperature |
| $T_{Com}$ | Temperature measurement of $Com$ |
| $T_{Com,A}$ | Lower threshold $Com$'s critical temperature range |
| $T_{Com,NF}$ | Upper threshold $Com$'s critical temperature range |
| $w_i$ | Priority of subsystem $i$ |
| $W_j$ | Rule firing strength of rule $j$ |
| $z_j$ | Rule output level of rule $j$ |

## I. INTRODUCTION

ELECTRIFICATION of transportation is a rapidly growing paradigm shift towards more efficient power and energy management, higher performance, and reliable vehicles. Hybridization of vehicle powertrains allow for optimization of the propulsive energy of the vehicle by effectively utilizing two or more power sources and achieve higher mileage and power capabilities while reducing greenhouse gas emissions [1]. Hybrid electric vehicle (HEV) power systems comprise of heterogeneous sources and demands, and their operating points affect individual components differently. It leads to have components at different states of health. Prolonged operation may result in lower efficiency and reliability, and it can also lead to system failures. For instance, heat waves in India have caused a large number of electrical vehicles to catch fire in April/ May 2022 [2]. Rising battery temperature, and their inability to dissipate heat during prolonged operation has caused fires. Typical energy management systems are based on electrical dynamics of the components that make up the system [3], [4], [5]. However, a component's performance depends on two other types of dynamics, namely, thermal and aging [6]. Situational awareness (SA) on two types of component dynamics are required to dispatch the component reliably.

SA is the perception of the elements in the environment within a volume of time and space, the comprehension of their meaning, and the projection of their status in the near future [7]. SA has gained popularity in a number of domains with critical operations, including military, aviation, air traffic control and power system. In each of these domains, a massive amount of data is received, and critical decisions are needed to be made fast, often by a human. Therefore, data should be converted to valuable information that could be comprehended by a human. For HEVs, such information facilitates effective decision making to ensure reliable and efficient operation.

The series HEV power system (Fig.1) uses both internal combustion engine and energy storage to meet system requirements such as vehicle range, charging/ fueling time and efficiency [8]. In [9], an integrated energy management and control (EMC) framework for a HEV was proposed. The framework is based on SA inferred using measurements of the vehicle power system (VPS) components (Fig. 2). SA can be used to dynamically reconfigure VPS components' operating states, and adaptations are proposed to the energy management system (EMS) based on SA levels.

The VPS in Fig. 2 is divided into subsystem based on functional contribution of subsets of the system, and these subsystems comprise of components. The components' functionality affect hierarchically subsystems' and system's functionality. Therefore, SA on functionality of each entity (components, subsystems and the system) is required to sustainably utilize them. In this study, authors define SA in the context of functionality as functional situational awareness (FSA).

FSA provides functionality information of components in VPS using measurements, and they can be used to dispatch decisions as depicted in Fig. 2. The EMC framework in the figure illustrates the interactions between different modules, namely, VPS, FSA, system mode of operation (SMO) and the dynamic optimization. It uses FSA to identify prevailing SMO, and dynamically optimize and dispatch energy resources. The SMO identifies VPS states as normal, critical and degraded. The identification of system mode assists dynamic optimization to adapt to prevailing system situation. FSA and SMO are used in the dispatch decision optimization. EMS receives objectives set by the operator and provide the performance index evaluations to the operator. The FSA based EMC framework's dual benefits are reliability and longevity of the VPS.

The contributions of this paper are as follows:

- A hierarchical FSA framework for VPS is proposed. FSA is inferred for different complexity levels (components, subsystems and system), and two types of inferences are defined: qualitative and quantitative. The knowledge depth increases with the Type as depicted in Fig. 3. FSA systems for components, subsystems and system are depicted in Figs. 4, 5 and 7, respectively.
- The hierarchical VPS-FSA framework is illustrated on an HEV power system. VPS is divided into subsystems based on functionality contribution to the overall vehicle power system. Fig. 2 illustrates the vehicle power system, and contribution of FSA to vehicle energy management system.

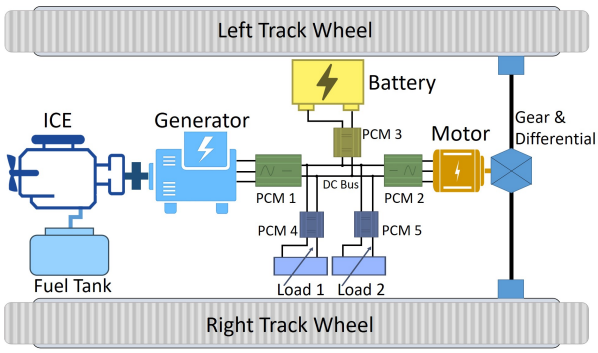


**FIGURE 1:** Powertrain of the HEV.

The rest of the paper is organized as follows: Section II introduces the HEV power system and thermal modeling. Section III elaborates FSA implementation steps in an HEV power system including component-FSA (in Section III-A), subsystem-FSA (in Section III-B) and system-FSA (in Section III-C). Section IV present the results and discussion of the case study. Finally, section V concludes the paper.

## II. HYBRID ELECTRIC VEHICLE POWER SYSTEM

In this study, an HEV is used to demonstrate the hierarchical FSA inference. The vehicle power system architecture is shown in Fig. 2.

### A. HEV POWERTRAIN

The HEV used in this study has a series powertrain as shown in Fig.1. A series hybrid is one in which the power converter only supplies the motor with propulsion power; the engine is no longer directly linked to the axis in this arrangement.Here, the generator, motor, battery storage and loads are connected to a DC bus through PCMs. The engine power is transformed into electrical energy by the generator, which can either run the motor directly or recharge the battery. The motor can be run solely on battery power, generator power, or a combination of both.

### B. HEV SYSTEM ARCHITECTURE

The HEV consists of five subsystems as follows:

- Subsystem 1: Internal combustion engine is located in this subsystem. It consists of two electrical power components, namely, generator and power conversion module (AC-DC). Generator is modeled as a three phase permanent magnet synchronous machine.
- Subsystem 2: Propulsion of the vehicle is located in subsystem 2, and it consists of the electric motors and power conversion modules (AC to DC). Motor is modeled as a three phase permanent magnet synchronous machine.
- Subsystem 3: Subsystem 3 is the energy storage subsystem. It consists of battery energy storage and power conversion module (DC-DC).
- Subsystem 4: Subsystem 4 consists of a constant power load critical electrical load dispatched during vehicle idle times. Only the power converter module is modeled with power data is provided to the model as an input.
- Subsystem 5: Subsystem 5 consists of cooling load for the entire vehicle, and only the power converter module is modeled with power data is provided to the model as an input.

Thermal characteristics of components can be learned by approximating them into a lumped parameter model, and using parameter identification methods. Thermal characteristics of the components are modeled using a lumped capacitance model [10], [11], [12], [13] as follows:

$$\frac{\partial T_{com}}{\partial t}(t) = a_{com} \times (Q_{l,com}(t) - Q_{c,com}(t) - b_{com} \times (T_{com}(t) - T_{amb}(t))) \quad (1)$$

$Q_{l,com}$ is computed using power loss of the equipment. Component efficiency is assumed to be linearly decreased with increasing degradation as follows:

$$Q_{l,com}(t) = ((1 - D_{com}(t)) \times \eta_{ini,com} + D_{com}(t) \times \eta_{fin,com}) \times P_{com}(t) \times \Delta t \quad (2)$$

Thermal coefficients ($a_{com}$ and $b_{com}$) used for the vehicle power system simulation are listed in Table 1.

**TABLE 1:** Coefficient values of components' thermal models [14].

| Component | $a_{com}$ | $b_{com}$ |
|---|---|---|
| PCM1 | 0.002 | 0.02 |
| Generator | 0.001 | 0.03 |
| PCM2 | 0.003 | 0.03 |
| Motor | 0.0006 | 0.05 |
| PCM3 | 0.002 | 0.02 |
| Battery | 0.0067 | 0.01 |
| PCM4 | 0.0015 | 0.02 |
| PCM5 | 0.0005 | 0.02 |

## III. FSA IMPLEMENTATION IN HEV POWER SYSTEM

Each component in an HEV has a unique contribution to the overall functionality of the vehicle power system. A subsystem, in this study, consists of multiple components and represents an energy resource. For instance, energy storage subsystem consists of battery that stores energy, PCM that convert electricity from battery voltage to the bus voltage. In a subsystem, components are integrated as a chain. Therefore, each component handles an equal amount of power (except the power loss).

However, power flow in the chain of components affect differently to each component. This is due to differences in efficiencies, heat removal process (natural, forced, rejection rate), construction and material properties. Therefore, a fusion of individual component-FSA inference is needed to evaluate subsystem-FSA. Similarly, characteristics of subsystems differ from eachother due to varying underlying

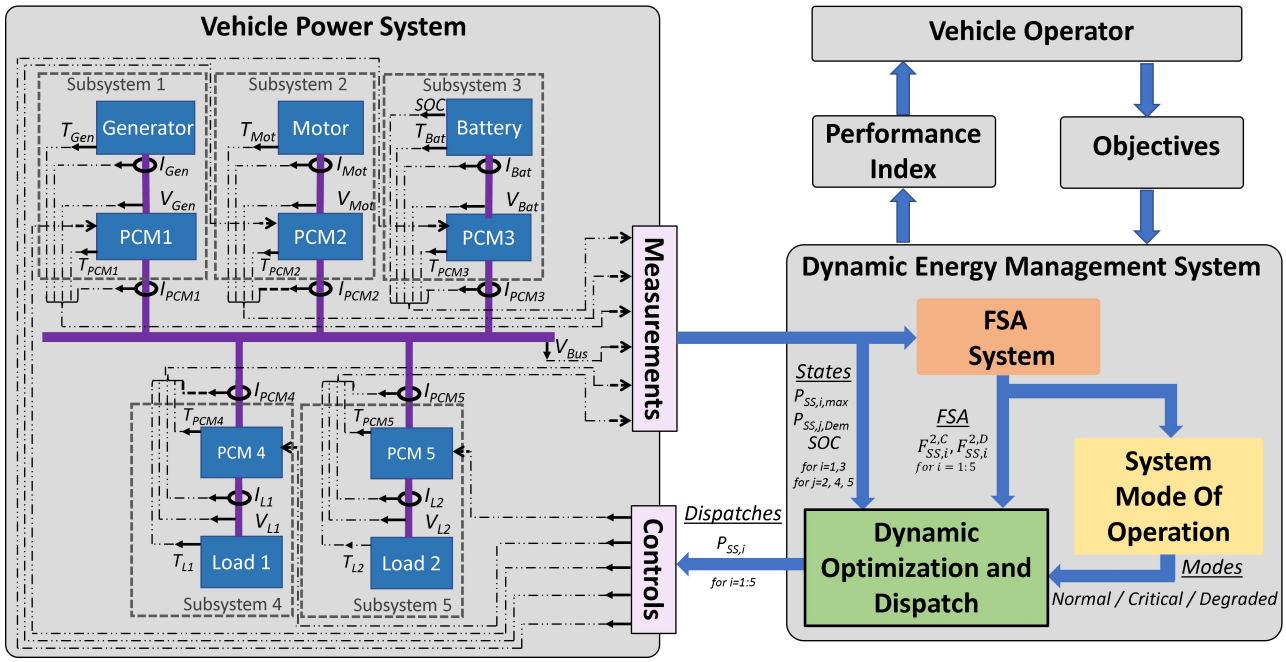


**FIGURE 2:** Energy management and control framework of an HEV with data and control flow shown.

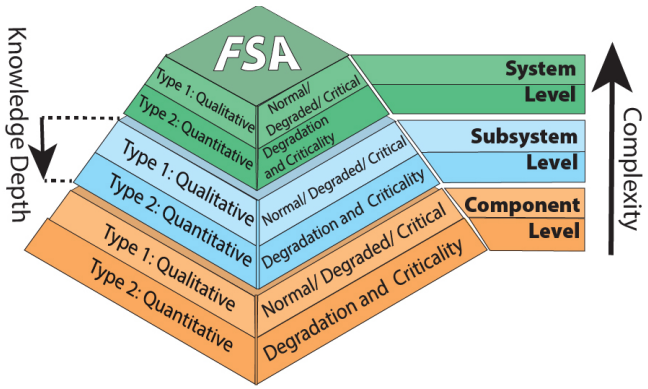


**FIGURE 3:** Complexity and knowledge depth of FSA system.

technologies and subsystems' utility to the system performance. Hence, system-FSA depends on subsystem-FSA, and is inferred as a fusion of subsystem-FSA.

FSA in each level (component, subsystem and system) inferred in two types. Entities are categorized into three states in Type 1-FSA estimation, namely, normal, degraded and critical. A normal state means the current operating conditions does not impact the functional capability of the entity and the full capacity is available to be dispatched.

Degraded and critical states indicate a compromise in the entity. Degraded state signifies lifetime compromise of the entity since the first use. Therefore, it is a non-decreasing function over time. On the other hand, critical state shows a compromise of the current operation. Type 2-FSA is conducted for entities in degraded and critical states. It assigns a value between 0 and 1 for each state.

### A. COMPONENT-FSA

Modern development in sensor technologies, communication and electronic circuitry have made many measurements available in components. These are essential in monitoring and control of the component and the power system as a whole. However, processing of measurements can produce more valuable insights to identify underlying dynamics. In this study, a fusion of measurements is carried out to provide functionality information of the component.

Components' Type 2-FSA are derived by comparing threshold values of the measurements/ metrics. Fig. 4 depicts the determination of component-FSA. Temperature and current of the component are used to determine whether the component is functional. Normal, critical and degraded states are defined based on threshold values of the measurements.

For components in critical/ degraded states, Type 2-FSA evaluation conducted using further analysis. Out of the components in a HEV power system, battery storage has the notion of capacity fading due to cycling. Hence, battery degradation is depicted in terms of capacity loss. In [15], Arrhenius equation [16] is used to model battery cycling and calendar degradation, and battery degradation has the following form:

$$D_{Bat} = \int_0^t \Delta D_{Bat} dt \tag{3}$$

$$\Delta D_{Bat} = \Delta D_{Bat,cyc} + \Delta D_{Bat,cal} \tag{4}$$

$$\Delta D_{Bat,cyc}(I_{Bat}, T_{Bat}) = f_1(I_{Bat}, T_{Bat}) \times e^{f_2(I_{Bat}, T_{Bat})} \tag{5}$$

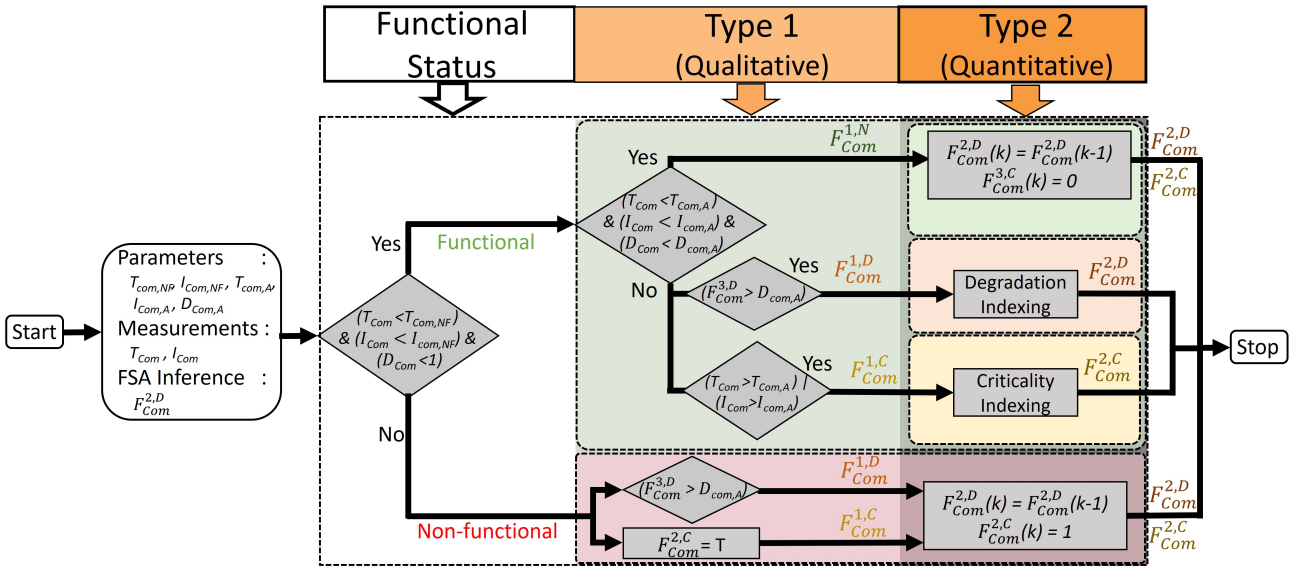


**FIGURE 4:** Component-FSA flowchart for two FSA Types (qualitative and quantitative).

$$\Delta D_{Bat,cal}(SOC, T_{Bat}, t) = f_3(SOC) \times e^{f_4(T_{Bat})} \times t^{0.5} \tag{6}$$

$f_1$, $f_2$, $f_3$ and $f_4$ are functions of respective variables which are determined through experiments.

For battery, a criticality metric is defined based on deviation of standard operating conditions such as temperature and current. The criticality depends less on calendar aging as it is slower than cycling aging (during use). Therefore, the criticality metric is defined as follows:

$$C_{Bat} = \frac{|\Delta D_{Bat}(I_{Bat}, T_{Bat}) - \Delta D_{Bat}(I_{Bat,C}, T_{Bat,C})|}{\Delta D_{Bat}(I_{Bat,NF}, T_{Bat,NF}) - \Delta D_{Bat}(I_{Bat,C}, T_{Bat,C})} \tag{7}$$

Electrical machines and power converters do not have a direct metric of degradation such as capacity fading in battery energy storage. However, there are stochastic models studied under prognostic health management. Such models estimate the remaining useful life of the components based on measurements [17]. Measurements are used to either estimate component parameters (such as internal resistance) or learn a function approximator to predict degradation/ remaining useful life. In this study, a linear combination of temperature and current is used to approximate criticality of machines and converters as follows:

$$C_{com} = \frac{\alpha_{com} \times I_{com,N} + \beta_{com} \times T_{com,N}}{\alpha_{com} + \beta_{com}} \tag{8}$$

$$I_{com,N} = \frac{I_{com} - I_{com,C}}{I_{com,NF} - I_{com,C}} \tag{9}$$

$$T_{com,N} = \frac{T_{com} - T_{com,C}}{T_{com,NF} - T_{com,C}} \tag{10}$$

Similar to battery, degradation is computed as an accumulation of criticality. Hence, integral of $C_{com}$ is considered as the degradation as follows:

$$D_{com} = k_{com} \times \int_0^t C_{com} dt \tag{11}$$

Components' criticality and degradation are evaluated using (8) and (11) in the absence of a degradation model. The coefficients $\alpha_{com}$ and $\beta_{com}$ determine relative contributions of current and temperature to aging of components.

### B. SUBSYSTEM-FSA

In the hierarchical VPS-FSA framework, component-FSA is the initial inference based on measurements. FSA of levels upward in the hierarchy, namely, subsystem and system are inferred based on FSA output of the previous level. It utilizes a logical fusion of previous level FSA output.

A subsystem represent an energy resource/ demand which comprises of multiple components. Therefore, FSA of energy resource/ demand is inferred using component-FSA in the subsystem. In this study, subsystem-FSA evaluations are done for two Types similar to components. Type 1-FSA evaluation is conducted using a simple logic that takes Type 1-FSA of components as depicted in Fig. 5.

In a subsystem, Functional Status is inferred using component Functional Status. As all the components in a subsystem are connected as a chain, non-functionality of any component leads to non-functionality of the subsystem. Using a similar reasoning, it can be concluded that both components should be in normal (Type 1-FSA) state to have a normal subsystem Type 1-FSA. If both components in the subsystem are not in normal states, the subsystem is in a degraded or critical (or both) state(s). Degraded/ critical (Type 1-FSA) of at least one of the components make the subsystem degraded/ critical.

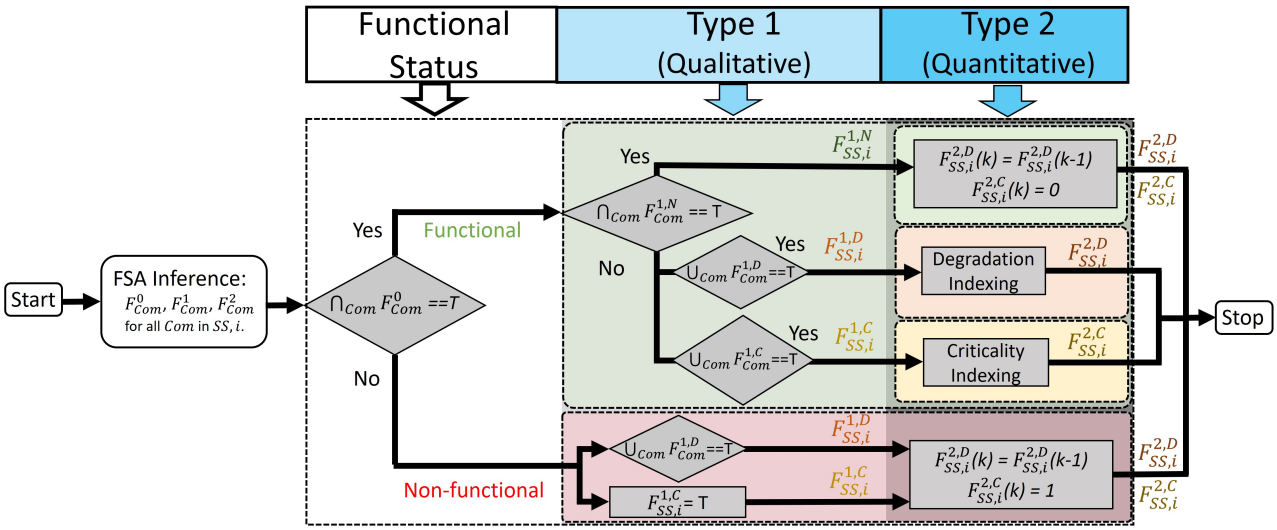


**FIGURE 5:** Subsystem-FSA flowchart for two FSA Types (qualitative and quantitative).

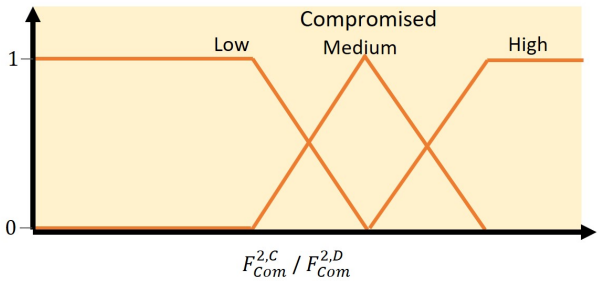


**FIGURE 6:** Input membership functions of FIS

In Type 2-FSA, quantitative inferences are done to determine degradation and criticality. In subsystems, criticality cannot be estimated directly similar to components. It can only be expressed quantitatively, possibly by an expert, with domain knowledge in the component technologies. A fuzzy inference system (FIS) is to infer these quantitative assessments to determine crisp levels of criticality and degradation. Fuzzy logic implements a mathematical model based on approximate reasoning. Fuzzy inference is the process of non-linear mapping a set of inputs to desired outputs using fuzzy logic.

In this study, FISs are used for criticality and degradation inferences in subsystems. Components' Type 2-Criticality and Degradation FSA are used as inputs to Takagi-Sugeno FIS [18]. Rules are defined for membership function combinations, and FIS is trained to map those instances. Type 2-Criticality FSA is inferred using components' criticality and degradation. For instance, in an energy storage subsystem, there are four inputs related to criticality and degradation (Type 2-FSA) of PCM and battery. Each input is fuzzified accordig to the three input membership functions shown in Fig. 6.Then the The inference technique involves reasoning using predefined fuzzy logic rules.There are 81 rules in the rule base ($3^4$). For degradation, only component degradations are used as FIS inputs, and 9 ($3^2$) rules are defined. The formulation of the fuzzy system to derive the subsystem level criticality and degradation is as follows:

$$F^{2,C}_{SS,i} = \frac{\sum_{j=1}^{81} W_j \times z_j}{\sum_{j=1}^{81} W_j} \tag{12}$$

$$F^{2,D}_{SS,i} = \frac{\sum_{j=1}^{9} W_j \times z_j}{\sum_{j=1}^{9} W_j} \tag{13}$$

### C. SYSTEM-FSA

Subsystems in HEV are connected radially, and consists of subsystems with power generators, energy storage and power demand. Therefore, unlike in a subsystem, Functional Status of the system does not require all the subsystems to be functional as depicted in Fig. 7. It requires at least one energy supply source (generator or energy storage) and at least one critical demand available. It is trivial that there should be at least one energy supply to function a vehicle power system. Type 1-FSA is similar to subsystem-FSA as the system is normal only when all the subsystems are normal and so on.

Subsystems in the system have different priorities depending on their utility to the system objectives. Therefore, a single degradation and criticality metric is computed for the collection of subsystems by weighting according to the priority. The formulation of system level criticality is as follows:

$$F^{2,C}_{Sys} = \frac{\sum F^{2,C}_{SS,i} \times w_i}{\sum w_i} \tag{14}$$

$$F^{2,D}_{Sys} = \frac{\sum F^{2,D}_{SS,i} \times w_i}{\sum w_i} \tag{15}$$

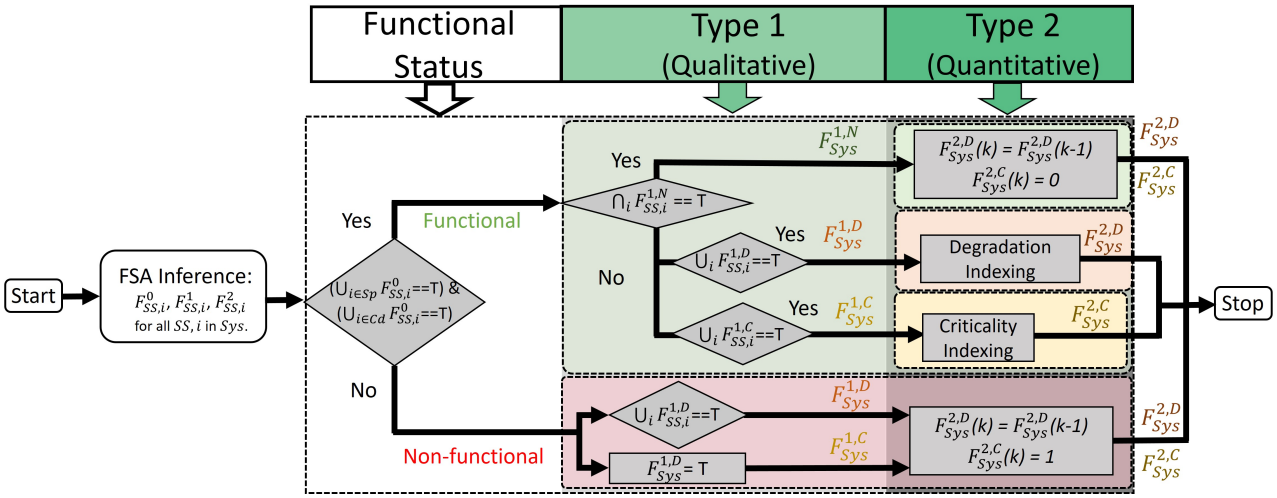


**FIGURE 7:** System-FSA flowchart for two FSA Types (qualitative and quantitative).

## IV. RESULTS AND DISCUSSION

The proposed hierarchical VPS-FSA framework is implemented on a HEV power system. Component-FSA is inferred using current $I_{com}$ and temperature $T_{com}$ measurements, and hierarchically for subsystems and system as discussed in Sections III-A, III-B and III-C.

Fig. 8 depicts the Urban Cycle 1 drive cycle [19] and power profiles for five subsystems (Fig. 2). The propulsion power requirement (Fig. 8c) generally depends on the acceleration and the maximum speed. This drive cycle demonstrates three sections of increasing power requirements. In the first stage, vehicle speed rises to 15 $kmph$ in an acceleration of 1 $ms^{-2}$. In the next two stages, the vehicle speed rises to 32 $kmph$ and 50 $kmph$, respectively. The accelerations are 0.69 $ms^{-2}$ and 0.55 $ms^{-2}$, respectively.

Component current measurements for the first run of the drive cycle are shown in Fig. 9. Current profiles are unique to the power demand/ supply of individual component. Temperature results are obtained by repeating the drive cycle multiple times, and results are depicted in Fig. 10 for $1^{st}$, $101^{st}$ and $201^{st}$ cycle. Temperature profiles of components depend on component efficiencies and heat removal process as shown in eq. 1. It should be noted that these thermal dynamics are unique for the drive cycle and system specifications.

In practical operation, a vehicle operator would pay attention to the system-FSA first, and look if the vehicle is functional and its Type 1 states. For $F^{1,C}_{Sys} == T$ or $F^{1,D}_{Sys} == T$, $F^{2,C}_{Sys}$ and $F^{2,D}_{Sys}$ indices will be analysed to estimate the degree of compromise. In such situations, the operator would scrutinize subsystem-FSA to find out what subsystems contributed to the prevailing compromise, and understand the component(s) in compromised subsystems those need attention. Depending on the severity of the component's functional capability and its impact to the current operation, objectives will be adjusted. Results are presented for the

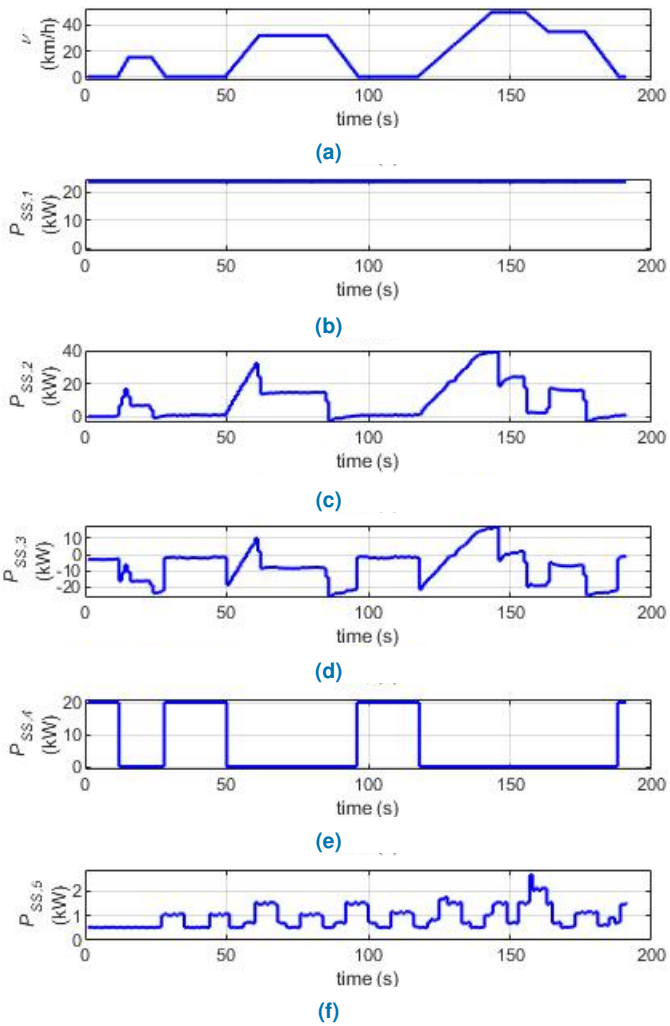


**FIGURE 8:** Drive cycle and power profiles of five subsystems: a) Urban Drive Cycle [19], b) engine power, c) propulsion power, d)energy storage power (discharging positive), e) load 1 power, f) load 2 power.

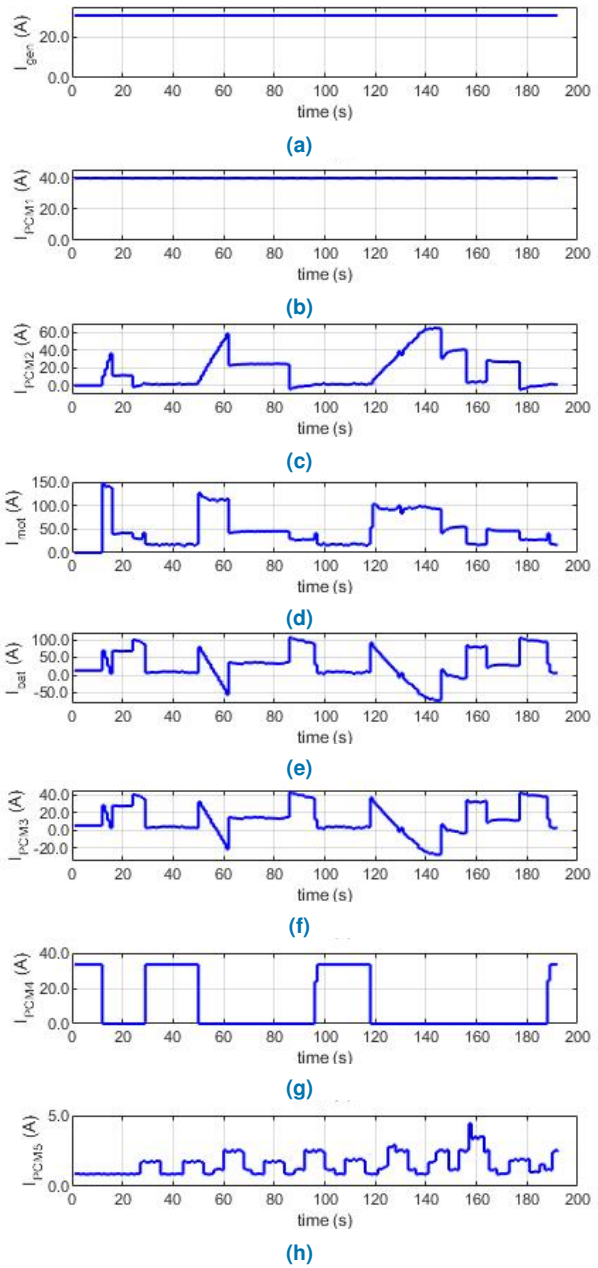


**FIGURE 9:** Components' current measurements: a) Generator ($I_{Gen}$), b) PCM1 ($I_{PCM1}$), c) PCM2 ($I_{PCM2}$), d) Motor ($I_{Mot}$), e) Battery ($I_{Bat}$), f) PCM3 ($I_{PCM3}$), g) PCM4 ($I_{PCM4}$), h) PCM5 ($I_{MCM5}$).

first drive cycle in that logical order: system, subsystem and component.

### A. SYSTEM-FSA

System-FSA is the holistic functionality indicator of the vehicle, and it conveys a summary of overall vehicle functional capability. Type 1-FSA depict any compromise in terms of critical and degraded states, and Type 2-FSA provides quantitative assessments of compromise in critical and degraded states. FSA provides alert signals if the system is in a compromised state to make necessary adjustment to sustain

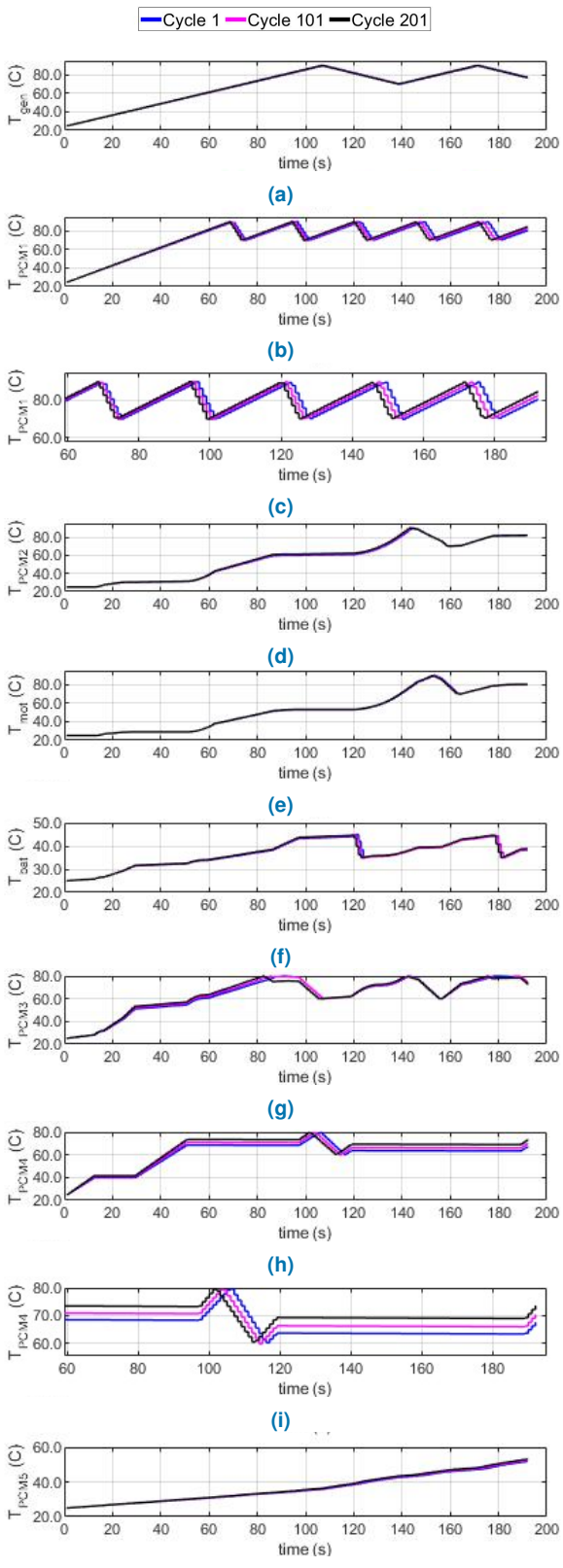


**FIGURE 10:** Components' temperature measurements: a) Generator ($T_{Gen}$), b) PCM1 ($T_{PCM1}$), c) PCM1 magnified ($T_{PCM1}$), d) PCM2 ($T_{PCM2}$), e) Motor ($T_{Mot}$), f) Battery ($T_{Bat}$), g) PCM3 ($T_{PCM3}$), h) PCM4 ($T_{PCM4}$), i) PCM4 magnified ($T_{PCM4}$), j) PCM5 ($T_{PCM5}$).

current operation.

Fig. 11 depicts system-FSA results for the first drive cycle. Type 1 stays normal for first 5 seconds, and changes to critical afterwards. Overall system degradation rises from zero. A comparison of results for $1^{st}$, $101^{st}$ and $201^{st}$ cycles are provided for Type 2-FSA by running the same cycle repeatedly. It is clearly seen that Criticality increases with the system degradation. In Fig. 11d the difference of the system degradation is plotted for 100 cycles. The results show that the degradation of the second 100 cycles is higher than the first. This illustrates the compounding effects of Criticality on Degradation.

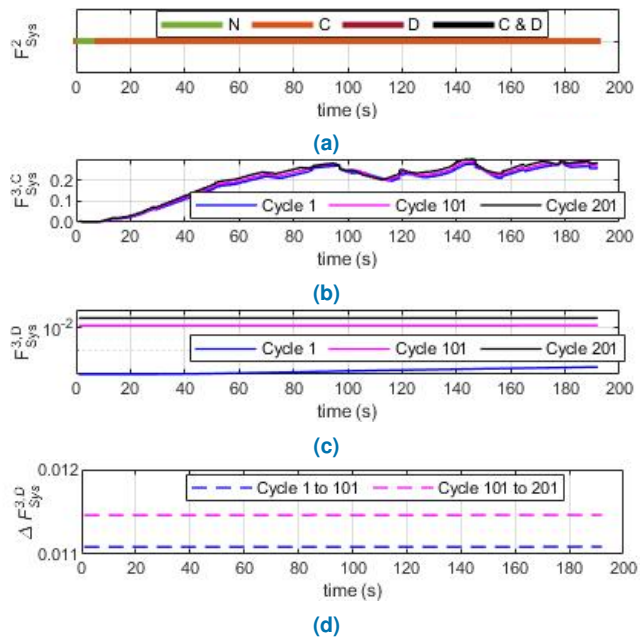


**FIGURE 11:** System-FSA results: a) Type 1, b) Type 2 - Degradation, c) Type 2 - Criticality, d) Degradation for 100 cycles.

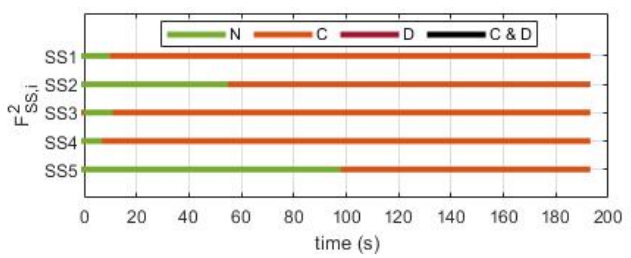


**FIGURE 12:** Subsystems' Type 1-FSA (N: Normal, C: Critical, D: Degraded).

### B. SUBSYSTEM-FSA

Subsystem-FSA is used to demonstrate functional capability of a particular energy resource or demand. It provides additional information related to a compromise in the system level. For instance, in Fig. 11a, the system becomes critical after 5 seconds approximately, and peaks (to 0.3 approx.) multiple times during the drive cycle. Subsystem-FSA can be used to infer more insights on subsystems that cause such compromises to the system.

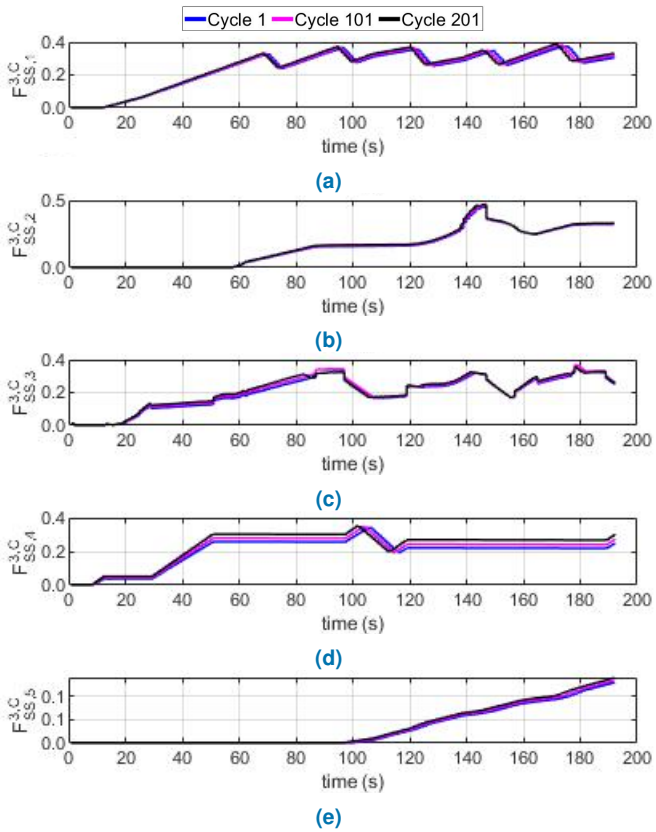


**FIGURE 13:** Subsystems' Type 2-Criticality FSA results: a) $SS, 1$, b) $SS, 2$, c) $SS, 3$, d) $SS, 4$, e) $SS, 5$.

Type 1-FSA is shown in Fig. 12. Subsystems attain normal and critical states only. This is because of new condition of the vehicle and degradation is lower than the threshold for degraded states.

Results in Fig. 13 illustrates criticality of different subsystems over time. For instance, subsystems 1 and 3 has criticality values between 0.2 and 0.4 after the rise from the initial values (zero). However, subsystem 3 criticality peaks around 145s to 0.5 approximately. Subsystems' degradations are depicted in Fig. 14 in a logarithmic scale. Components' contribution to subsystems' criticality and degradation can be analysed using components' FSA data.

### C. COMPONENT-FSA

Components are the interfaces of the FSA to the physical system via measurements. Similar to subsystems, components' Type 1-FSA (Fig. 15) attains normal and critical states only. Type 3-Criticality and Degradation results of the components are shown in Figs. 16 and 17 respectively. In Fig.13a, Type 2-Criticality FSA for$SS, 1$ depicted, and it shows a periodic rise and fall of the criticality index. The observation in Fig.16b of Type 2-Criticality FSA for components in $SS, 1$ proves that the subsystem criticality is mainly contributed by

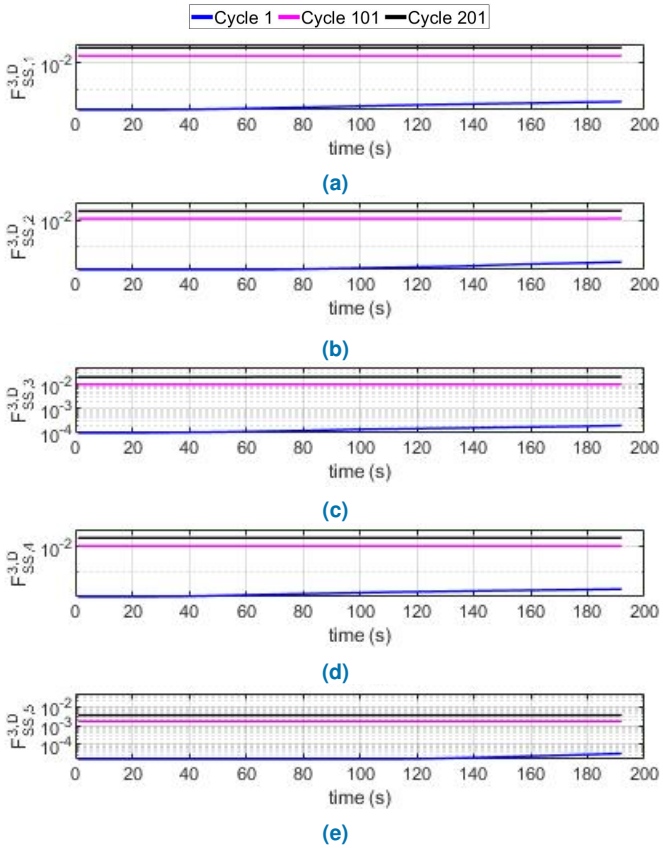


**FIGURE 14:** Subsystems' Type 2-Degradation FSA results: a) $SS,1$, b) $SS,2$, c) $SS,3$, d) $SS,4$, e) $SS,5$.

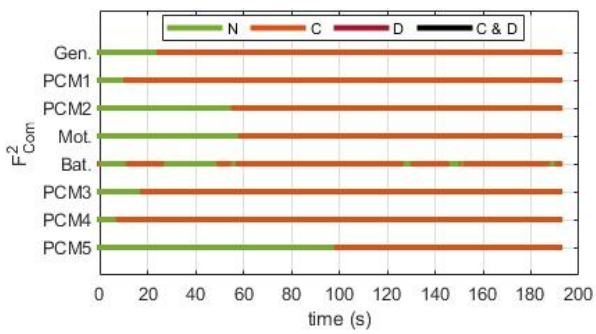


**FIGURE 15:** Components' Type 1-FSA (N: Normal, C: Critical, D: Degraded).

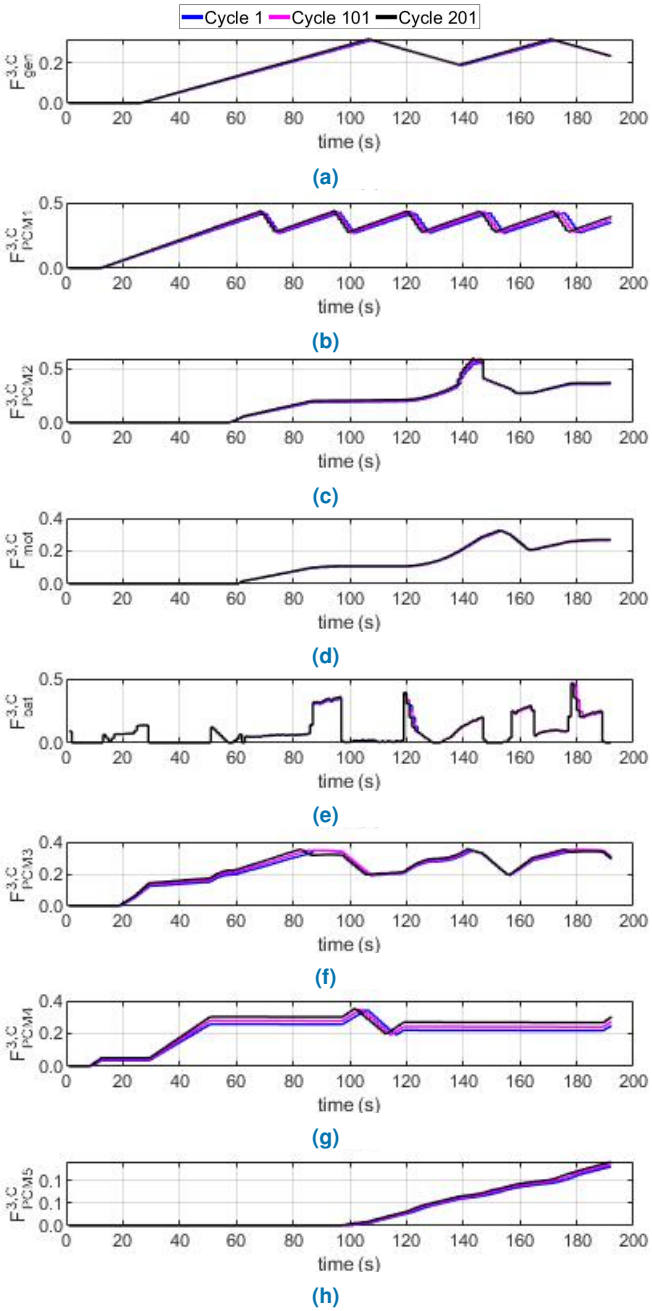


**FIGURE 16:** Components' Type 2-Criticality FSA results: a) Generator, b) PCM1, c) PCM2, d) Motor, e) Battery, f) PCM3, g) PCM4, h) PCM5.

$PCM1$. The periodic behavior of the criticality is coming from the thermostat operation of component cooling. On the other hand, as shown in Fig.16c criticality FSA for $SS,2$ components reach their peaks close to 150s though $PCM2$ reaches a higher peak. This is due to the higher propulsion power demand during high acceleration and velocity.

The battery criticality depicted in Fig. 16e shows a more complex behavior. This is due to the exponential equations in criticality and degradation modeling of Lithium-ion batteries. $PCM$s are the only electrical components in $SS,4$ and $SS,5$. Therefore, they solely contribute to their respective subsystem-FSA.

### D. DISCUSSION

The results presented demonstrate increasing complexity in bottom-up hierarchy. The component-FSA is simpler and can be inferred using the component's measurements. However, in two upper levels of the hierarchy, FSA can be only inferred by fusing FSA of the previous level. Therefore, components are connected together to form a tree-like structure in hierarchical FSA inference. In subsystem-FSA, a dominant component that contributes to subsystem-FSA can be singled out. The differentiating factors for the components' behavior

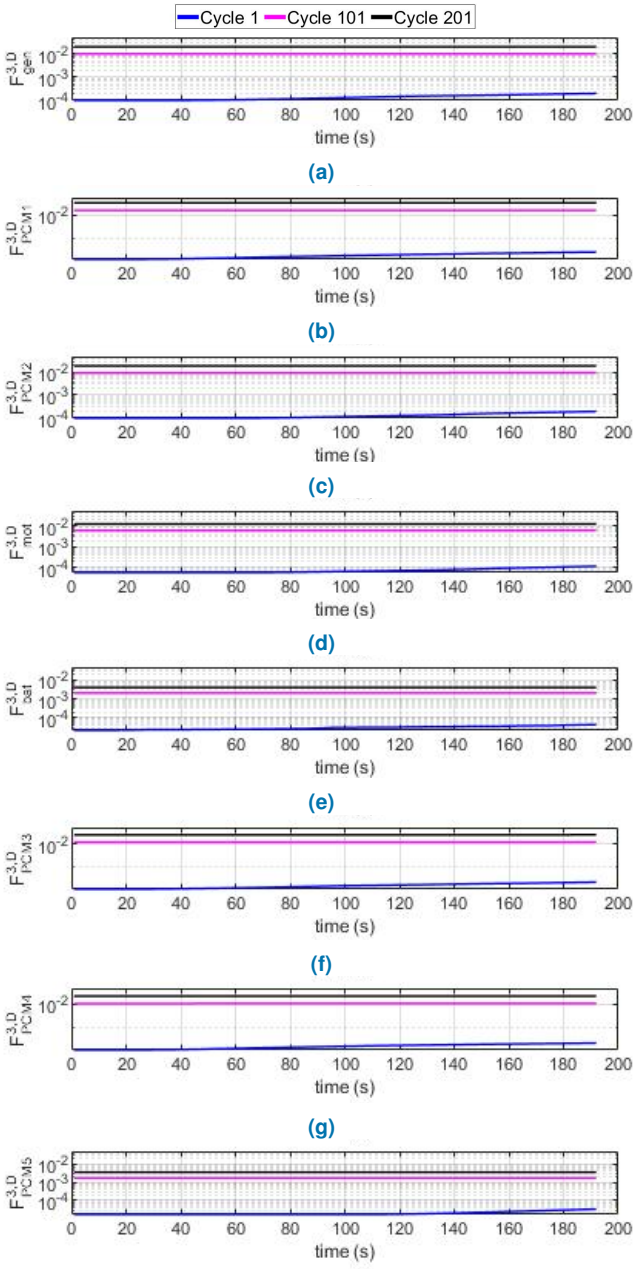


**FIGURE 17:** Components' Type 2-Degradation FSA results: a) Generator, b) PCM1, c) PCM2, d) Motor, e) Battery, f) PCM3, g) PCM4, h) PCM5.

are technical specifications (electrical and thermal) and heat removal process. A more combined effect is demonstrated in system-FSA where all the subsystems are integrated based on the functional priority.

In Table 2, criticality and degradation results are compared for the system, subsystem and component levels at different number of cycles. The results are achieved by running Urban Cycle 1 drive cycle repeatedly. The results indicated are the maximum values during the cycle. Though the results are derived by running the same drive cycle, criticality values are increasing over time. For instance, the system criticality reaches a peak of 0.2812 during the first cycle, and gradually increases to 0.3492 in the 801st cycles. Therefore, degradation also increases with criticality in a compounded manner, and the energy management system should take the degradation into account in order to maintain the functional capability of the vehicle power system.

It is observed that subsystem 2 and its components' Type 2-Criticality FSA is higher than other subsystems. However, its degradation is not the highest among five subsystems. This is a result of its components' temperature and current variations during the drive cycle. For instance, as shown in Figs. 9c and 10d, $PCM2$ current and temperature reach their peaks around 145s. The current is rising and falling (as observed in Fig. 9(c)) according to the drive cycle in Fig. 8(a). The different peaks in the current are based on the different vehicle speeds. However, the temperature is increasing during the drive cycle until around 145 s and then drops (as observed in Fig. 10(d)).

In this study, component temperatures are controlled by dual-setpoint thermostat cooling. In the simulation, $PCM2$ and $Mot$ (subsystem2 components) are maintained between 70-90 Celcius during thermostat control for the base study. An additional study is conducted to evaluate the effects of thermostat setpoints on Type 2-FSA for subsystem 2 and its components by reducing thermostat temperature range to 60-80 Celcius. Results are shown in Table 3. It is evident that the drop in thermostat dual-setpoints reduce both Criticality and Degradation of subsystem 2 and its components. This result highlights the importance temperature control in components for a reliable VPS.

The importance of FSA in a VPS is presented in this paper. However, the full potential of VPS-FSA framework can only be reaped by deploying it in energy management and control of VPS. Energy management and control of HEV should be further investigated based on FSA as depicted in Fig. 2.

## V. CONCLUSION

In this paper, functional situational awareness (FSA) is introduced to infer functionality of a hybrid electric vehicle power system (VPS). VPS-FSA framework uses measurements as inputs to derive FSA at three hierarchical levels, namely, component, subsystem and system. In component level, current and temperature measurements are used to identify component's functional capability. Subsystem-FSA is determined based on FSA of the components in energy resource's subsystem. Similarly, system-FSA is inferred as a fusion of subsystem-FSA.

Two types of FSA proposed in each stage. In Type 1, a binary qualitative evaluation is done to estimate whether the entity (component, subsystem or system) is functional. Functional entities are further categorized into three states, namely, normal, degraded and critical. Degraded and critical states signify a compromised condition of the entity and reduces available capacity of the entity for dispatch. Type 3-FSA inference is conducted for degraded and critical states

**TABLE 2:** Results summary of repeated simulation of Urban Cycle 1 drive cycle.

| Entity | | Type 3-FSA | Maximum value during the cycle | | | | | |
|---|---|---|---|---|---|---|---|---|
| | | | Cycle 1 | Cycle 101 | Cycle 201 | Cycle 401 | Cycle 601 | Cycle 801 |
| System | | Criticality | 0.2812 | 0.287 | 0.2999 | 0.3227 | 0.3356 | 0.3492 |
| | | Degradation | 0.0001 | 0.0113 | 0.0228 | 0.0462 | 0.0676 | 0.0886 |
| Subsystem 1 | | Criticality | 0.3762 | 0.3818 | 0.3900 | 0.3999 | 0.4117 | 0.4223 |
| | | Degradation | 0.0002 | 0.0185 | 0.0364 | 0.0701 | 0.1013 | 0.1301 |
| Subsystem 1 Components | Gen. | Criticality | 0.3127 | 0.3158 | 0.3190 | 0.3256 | 0.3328 | 0.3401 |
| | | Degradation | 0.0001 | 0.0097 | 0.0195 | 0.0394 | 0.0598 | 0.0807 |
| | PCM1 | Criticality | 0.4235 | 0.4297 | 0.4371 | 0.4523 | 0.4688 | 0.4879 |
| | | Degradation | 0.0002 | 0.0153 | 0.0309 | 0.0630 | 0.0965 | 0.1315 |
| Subsystem 2 | | Criticality | 0.4638 | 0.4653 | 0.4721 | 0.5016 | 0.5334 | 0.5697 |
| | | Degradation | 0.0001 | 0.0116 | 0.0231 | 0.0455 | 0.0672 | 0.0884 |
| Subsystem 2 Components | PCM2 | Criticality | 0.5610 | 0.5757 | 0.5916 | 0.6326 | 0.6762 | 0.7264 |
| | | Degradation | 0.0001 | 0.0095 | 0.0192 | 0.0395 | 0.0610 | 0.0837 |
| | Mot. | Criticality | 0.3239 | 0.3257 | 0.3275 | 0.3320 | 0.3362 | 0.3407 |
| | | Degradation | 0.0001 | 0.0060 | 0.0120 | 0.0243 | 0.0369 | 0.0497 |
| Subsystem 3 | | Criticality | 0.3645 | 0.3695 | 0.3712 | 0.3741 | 0.3775 | 0.3816 |
| | | Degradation | 0.0001 | 0.0099 | 0.0198 | 0.0396 | 0.0595 | 0.0796 |
| Subsystem 3 Components | Bat. | Criticality | 0.4751 | 0.4761 | 0.4776 | 0.4795 | 0.4826 | 0.4869 |
| | | Degradation | 0.0001 | 0.0021 | 0.0041 | 0.0083 | 0.0125 | 0.0168 |
| | PCM3 | Criticality | 0.3471 | 0.3519 | 0.3553 | 0.3646 | 0.3750 | 0.3987 |
| | | Degradation | 0.0001 | 0.0121 | 0.0244 | 0.0496 | 0.0757 | 0.1029 |
| Subsystem 4 (PCM4) | | Criticality | 0.3472 | 0.3504 | 0.3547 | 0.3656 | 0.3739 | 0.3830 |
| | | Degradation | 0.0001 | 0.0110 | 0.0230 | 0.0501 | 0.0719 | 0.0938 |
| Subsystem 5 (PCM5) | | Criticality | 0.1319 | 0.1367 | 0.1422 | 0.1534 | 0.1686 | 0.1859 |
| | | Degradation | 0.0000 | 0.0017 | 0.0036 | 0.0075 | 0.0119 | 0.0169 |

**TABLE 3:** Repeated cycles results with 10 Celsius lower thermostat dual-setpoint for subsystem 2 components.

| Entity | | Type 2-FSA | Maximum value during the cycle | | | | | |
|---|---|---|---|---|---|---|---|---|
| | | | Cycle 1 | Cycle 101 | Cycle 201 | Cycle 401 | Cycle 601 | Cycle 801 |
| Subsystem 2 | | Criticality | 0.2981 | 0.3000 | 0.3024 | 0.3066 | 0.3111 | 0.3163 |
| | | Degradation | 0.0001 | 0.0099 | 0.0195 | 0.0382 | 0.0562 | 0.0737 |
| Subsystem 2 Components | PCM2 | Criticality | 0.3474 | 0.3493 | 0.3527 | 0.3585 | 0.3648 | 0.3716 |
| | | Degradation | 0.0001 | 0.0080 | 0.0161 | 0.0325 | 0.0495 | 0.0669 |
| | Mot. | Criticality | 0.2658 | 0.2667 | 0.2675 | 0.2709 | 0.2735 | 0.2773 |
| | | Degradation | 0.0001 | 0.0051 | 0.0102 | 0.0204 | 0.0308 | 0.0414 |

which computes compromise in terms of degradation and criticality of the entity.

## REFERENCES

[1] J. Miller, "Hybrid electric vehicle propulsion system architectures of the e-cvt type," *IEEE Transactions on Power Electronics*, vol. 21, no. 3, pp. 756–767, 2006.

[2] S. Dinakar, "The burning question: Why are electric two-wheelers in india catching fire?" www.business-standard.com/article/companies/the-burning-question-why-are-electric-two-wheelers-in-india-catching-\fire-122050301202_1, 2022, 'Accessed: 2022-06-15'.

[3] Z. E. Liu, Q. Zhou, Y. Li, and S. Shuai, "An intelligent energy management strategy for hybrid vehicle with irrational actions using twin delayed deep deterministic policy gradient," *IFAC-PapersOnLine*, vol. 54, no. 10, pp. 546–551, 2021, 6th IFAC Conference on Engine Powertrain Control, Simulation and Modeling E-COSM 2021. [Online]. Available: https://www.sciencedirect.com/science/article/pii/S2405896321016219

[4] Q. Zhou, D. Zhao, B. Shuai, Y. Li, H. Williams, and H. Xu, "Knowledge implementation and transfer with an adaptive learning network for real-time power management of the plug-in hybrid vehicle," *IEEE Transactions on Neural Networks and Learning Systems*, vol. 32, no. 12, pp. 5298–5308, 2021.

[5] G. K. Venayagamoorthy, R. K. Sharma, P. K. Gautam, and A. Ahmadi, "Dynamic energy management system for a smart microgrid," *IEEE Transactions on Neural Networks and Learning Systems*, vol. 27, no. 8, pp. 1643–1656, 2016.

[6] L. Calearo, A. Thingvad, C. Ziras, and M. Marinelli, "A methodology to model and validate electro-thermal-aging dynamics of electric vehicle battery packs," 2021.

[7] M. R. Endsley, "Design and evaluation for situation awareness enhancement," *Proceedings of the Human Factors Society Annual Meeting*, vol. 32, no. 2, pp. 97–101, 1988. [Online]. Available: https://doi.org/10.1177/154193128803200221

[8] J. Manwell, "Hybrid energy systems," in *Encyclopedia of Energy*, C. J. Cleveland, Ed. New York: Elsevier, 2004, pp. 215–229. [Online]. Available: https://www.sciencedirect.com/science/article/pii/B012176480X003600

[9] G. K. Venayagamoorthy, C. Pathiravasam, P. Herath, H. Dharmawardena, D. Rizzo, and M. P. Castanier, "An integrated energy management and control framework for hybrid military vehicles based on situational awareness and dynamic reconfiguration," in *SAE Technical Paper 2022-01-0349*, 2022.

[10] B. Rodríguez, E. Sanjurjo, M. Tranchero, C. Romano, and F. González, "Thermal parameter and state estimation for digital twins of e-powertrain components," *IEEE Access*, vol. 9, pp. 97 384–97 400, 2021.

[11] S. Ahmed Abdelrahman and B. Bilgin, "Computationally efficient surrogate-based magneto-fluid-thermal numerical coupling approach for a water-cooled ipm traction motor," *IEEE Access*, vol. 10, pp. 83 692–83 704, 2022.

[12] S. H. Shah, X. Wang, M. Azeem, and U. Abubakar, "Coupled magnetic field and thermal analysis model for an ipmsm with modular three-phase winding topologies for fault-tolerant applications," *IEEE Access*, vol. 10, pp. 30 335–30 348, 2022.

[13] K. I. Alsharif, A. H. Pesch, V. Borra, F. X. Li, P. Cortes, E. Macdonald, and K. Choo, "A coupled thermo-mechanical dynamic characterization of cylindrical batteries," *IEEE Access*, vol. 10, pp. 51 708–51 722, 2022.

[14] S. Miller, "Hybrid-electric vehicle model in simulink," 2023, accessed: 2023-03-25. [Online]. Available: https://github.com/mathworks/Simscape-HEV-Series-Parallel/releases/tag/22.2.4.5

[15] D. Wang, J. Coignard, T. Zeng, C. Zhang, and S. Saxena, "Quantifying

electric vehicle battery degradation from driving vs. vehicle-to-grid services," *Journal of Power Sources*, vol. 332, pp. 193–203, 2016. [Online]. Available: https://www.sciencedirect.com/science/article/pii/S0378775316313052

[16] S. R. Logan, "The origin and status of the arrhenius equation," *Journal of Chemical Education*, vol. 59, no. 4, p. 279, 1982. [Online]. Available: https://doi.org/10.1021/ed059p279

[17] L. Saidi and M. Benbouzid, "Prognostics and health management of renewable energy systems: State of the art review, challenges, and trends," *Electronics*, vol. 10, no. 22, 2021. [Online]. Available: https://www.mdpi.com/2079-9292/10/22/2732

[18] J. H. Lilly, "Takagi-sugeno fuzzy systems," in *Fuzzy Control and Identification*. Wiley, 2010.

[19] "Dynamometer drive schedules," www.epa.gov/vehicle-and-fuel-emissions-testing/dynamometer-drive-schedules, 2022, 'Accessed: 2022-09-22'.

CHIRATH PATHIRAVASAM (S'15) received B. S. degree in electrical engineering from University of Moratuwa, Katubedda, Sri Lanka in 2011. He is currently pursuing the Ph.D. degree in electrical engineering at Clemson University, Clemson SC, USA. He has recently joined Eaton Research Lab as a Lead Engineer in the Grid Intelligence team. His research interests include multi-microgrid systems, grid intelligence, demand flexibility, distribution grid automation and energy management systems.

GANESH K. VENAYAGAMOORTHY (S'91-M'97-SM'02-F'21) received the B.Eng. degree (Hons.) in electrical and electronics engineering from Abubakar Tafawa Balewa University, Bauchi, Nigeria, in March 1994, the M.Sc.Eng. and Ph.D. degrees in electrical engineering from the University of Natal, Durban, South Africa, in April 1999 and April 2002, respectively, and the M.B.A. degree in entrepreneurship and innovation from Clemson University, Clemson, SC, USA, in August 2016.

From 1996 to 2002, he was a Senior Lecturer with the Department of Electronic Engineering, Durban University of Technology, Durban, South Africa. From 2002 to 2011, he was a Professor of electrical and computer engineering with the Missouri University of Science and Technology (Missouri S&T), Rolla, MO, USA. He was the Founder, in 2004, and the Director of the Real-Time Power and Intelligent Systems Laboratory. Since January 2012, he has been the Duke Energy Distinguished Professor of power engineering and a Professor of electrical and computer engineering with Clemson University. He led the Brain2Grid project funded by the U.S. National Science Foundation (NSF). He is an inventor of technologies for scalable computational intelligence for complex systems and dynamic stochastic optimal power flow. He has published $\sim$ 600 refereed technical articles which are cited $\sim$ 23,000 times with an H-index of 70 and i10-index of > 300. He has given over 500 invited technical presentations, including keynotes and plenaries in over 40 countries to date. His interests include research, development, and innovation in power systems, smart grid, and artificial intelligence (AI) technologies.

Dr. Venayagamoorthy is a Fellow of the Institution of Engineering and Technology (U.K.), the South African Institute of Electrical Engineers (SAIEE) and Asia-Pacific Artificial Intelligence Association (AAIA), and a Senior Member of the International Neural Network Society (INNS). He is a 2004 US NSF CAREER Awardee, a 2007 US Office of the Naval Research (ONR) Young Investigator Program (YIP) Awardee, and a 2008 NSF Emerging Frontiers in Research and Innovation (EFRI) Awardee. He has received several awards for faculty, research and teaching excellence from universities, professional societies, and organizations. According to a recent Stanford study, Dr. Venayagamoorthy is among the top 25,000 scientists worldwide across all fields and in the top 0.1% worldwide in the fields of energy and AI. He is involved in the leadership and organization of conferences, including the Clemson University Power System Conference and a Pioneer and the Chair/Co-Chair of the IEEE Symposium of Computational Intelligence Applications in Smart Grid (CIASG), since 2011. He is also the Chair of the IEEE PES Working Group on Intelligent Control Systems, and the Founder and the Chair of IEEE Computational Intelligence Society (CIS) Task Force on Smart Grid. Dr. Venayagamoorthy has served/serves as an Editor/Associate Editor/Guest Editor of several IEEE TRANSACTIONS and Elsevier journals and he is the Editor for the IEEE Press Series on Power and Energy Systems. He is an IEEE CIS and IES Distinguished Lecturer.

RAJAN RATNAKUMAR (S'19) received B.S. degree in electrical and electronic engineering from University of Jaffna, Jaffna, Sri Lanka in 2018. He is currently pursuing the Ph.D. degree in electrical engineering at Clemson University, Clemson SC, USA. He is a lecturer (probationary) at University of Jaffna, Faculty of Engineering since 2019 and is a research assistant at the Real-Time Power and Intelligent Laboratory in Clemson University from 2022 to present. His research interests include renewable energy generation and its integration, power system stability and control.

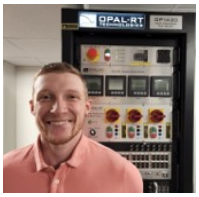

KYLE SKEEN (S'21) received a B.S. degree in Electrical Engineering and B.S. in Applied Mathematics from Western Carolina University, Cullowhee, NC, USA in 2021. Currently he is at Clemson University, Clemson, SC, USA pursuing a M.S. degree in Electrical Engineering and was with the Real-Time Power and Intelligent Systems (RTPIS) Laboratory, Clemson University. Research interests include microgrid controls, economic dispatch, and distributed energy resources (DERs).